GRAVITY EFFECT ON THE CATASTROPHIC DYNAMIC RESPONSE OF STRAIN-HARDENING MULTI-STORY FRAMES

by
Ryo Tanabashi*, Tsuneyoshi Nakamura**, and Shuzo Ishida***

SYNOPSIS

An efficient computational method of dynamic large-deflection analysis of elastic strain-hardening multi-story frames is developed in this paper. Both of the gravity effect and the effect of spreading and diminishing of strain-hardening regions are taken into account without increasing too greatly the size of computational time. It is shown through numerical examples that the method with an experimental verification on the considerably good accuracy of the member-stiffness equation, is able to predict the deteriorating process and the tendency of dynamical collapse behavior of multi-story building frames subjected to amplified strong-motion earthquake disturbances.

1. INTRODUCTION

Some of the recent earthquake records including those of the San Fernando Earthquake appear to show that earthquakes with ground accelerations and velocities of extremely high intensity have occurred even if their magnitudes may not have been great and to lead us to reconsider the maximum ground acceleration and velocity to be taken into account in the design of framed structures. In order to establish a rational method of earthquake resistant design of framed structures subjected to such ground acceleration and velocity of unknown high intensity, it is necessary to clarify to what intensities of ground acceleration and velocity a frame will not really collapse and therefore what strengths and ductilities the members of the frame must be assigned so as not to collapse under certain given ground motions.

The deteriorating process and dynamical collapse behavior of an actual steel frame can be investigated only if both of the gravity effect (the so-called PΔ-effect) and the strain-hardening effect , at least, are taken into account in the realistic simulation of the frame as a system of bar members. The latter effect favorable in the sense that the strain-hardening results in well-stable restoring-force characteristics, may be considerably decreased or cancelled by the former effect which would become more unfavorable as the horizontal displacements become greater. It is therefore necessary to develop a refined computational method of dynamic large-deflection analysis of strain-hardening frames such that gradual spreading and diminishing of strain-hardening regions along member axes are taken into account.

A great number of previous works on earthquake response analysis of inelastic building frames have been carried out mostly on the basis of

* Professor Emeritus of Kyoto University, Kyoto,
** Associate Professor of Architecture, Kyoto University, Kyoto,
*** Associate Professor of Architecture, Kyoto Technical University, Kyoto.

simplified models and model frames. Some of the recent investigations have dealt with more realistic frames with strain-hardening force-displacement characteristics[1] with some effort to take into account the gravity effect, while others with simplified one- and two-degree-of freedom models with the gravity effect in the idealization[2],[3]. It does not appear, however, that the gravity effect on the catastrophic dynamic response of strain-hardening multi-story frames has been clarified even for their simple multi-degree-of-freedom models. As far as multi-story frames consisting of elastic-plastic members are concerned, the gravity effect has been clarified only on the static load-deflection behaviors of elastic-perfectly plastic frames by the present authors[4],[5].

The purpose of the present paper is to propose an efficient computational method of dynamic large-deflection analysis of strain-hardening frames and to illustrate, through numerical examples, the deteriorating process and the tendency of dynamical collapse behavior of frames subjected to amplified strong-motion earthquake disturbances. The gravity effect on the elastic behavior of a frame can be assessed quantitatively if the well-known geometrical stiffness matrix is utilized. For a strain-hardening frame, gradual spreading and diminishing of strain-hardening regions under bending moment and axial force along member axes must all be taken into account. Any straight forward application of the finite element method for static large-deflection analysis of strain-hardening frames in which a member is subdivided into several elements, may of course be possible, if with a huge cost, so far as the capacity of available computers allows. The method proposed here, however, has been developed with the intention of minimum economy so that a number of parametric numerical investigations would become possible on an available computer such as FACOM 230-60 or IBM360.

The main features of the method may be summarized as follows:

(1) The transfer matrix technique is applied to the elements of a member as a subsystem to generate an accurate member-stiffness matrix and the stiffness method to the frame as a global system.
(2) Each member in the elastic region is treated as one element and then subdivided automatically in the program into as many elements as are necessary as the strain-hardening regions in the member spread over.

2. ASSUMPTIONS

The following assumptions are made in this paper besides the usual assumptions for in-plane analysis of a plane frame consisting of uniform prismatic straight members. Fig.1 shows the model frame considered here.

(1) A cross-section is idealized as an equivalent sandwich section consisting of two flanges with a concentrated area of half the actual area[7].
(2) Each flange obeys the bilinear hysteretic stress-strain relation.
(3) A lumped mass is placed only at each joint. The mass moment of inertia due to distributed mass of a beam is taken into account at each joint.
(4) The substructure is idealized as a rigid base connected with the base rock as shown in Fig.2 through a horizontal spring, a vertical spring, and a rotational spring and the corresponding dashpots representing the ground properties.
(5) Earthquake disturbances with horizontal and vertical components are introduced into the base rock.
(6) The damping matrix is proportional to the system stiffness matrix.

3. STIFFNESS MATRIX OF A MEMBER

One of the main features of the present method of analysis is the application of the transfer matrix technique to constituent individual beams and columns to derive the member-stiffness matrix. A member, either a beam or a column, is conceived, whenever necessary, as a subsystem consisting of several elements connected one-dimensionally along the member axis in sequence. Fig.3 shows the coordinates defined at the ends of a member and those for a typical element, where ξ and η are defined by $\xi = x/l$ and $\eta = z/l$, respectively.

Let $u(\xi)$ and $v(\xi)$ denote the tangential and normal displacement components of the point at ξ nondimensionalized with respect to l and measured in the local coordinate system (ξ, η) which is defined on the rotated but undeformed cantilever axis as shown in Fig.3. The slope at ξ in this local coordinate system is defined by $\theta(\xi) = dv/d\xi$. A small increment of a variable from a current value will be denoted by Δ. The following displacement functions are assumed for an element:

$$\begin{Bmatrix} \Delta u \\ \Delta v \\ \Delta\theta \end{Bmatrix} = \begin{bmatrix} \xi & 0 & 0 \\ 0 & \xi^2 & \xi^3 \\ 0 & 2\xi & 3\xi^2 \end{bmatrix} \begin{Bmatrix} \Delta\alpha_1 \\ \Delta\alpha_2 \\ \Delta\alpha_3 \end{Bmatrix} \quad \text{(1a)} \qquad \text{or} \quad \{\Delta d(\xi)\} = [\Gamma_\xi]\ \{\Delta\alpha\} \quad \text{(1b)}$$

where α_1, α_2 and α_3 are the usual generalized coordinates, which can be expressed in terms of the end displacement vector $\{\Delta d_a\}=\{\Delta u_a,\ \Delta v_a,\ \Delta\theta_a\}^T$ as follows:

$$\{\Delta\alpha\} = [\Gamma]^{-1}\{\Delta d_a\} \quad \text{(2)} \qquad \text{where} \quad [\Gamma]^{-1} = \begin{bmatrix} 1 & 0 & 0 \\ 0 & 3 & -1 \\ 0 & -2 & 1 \end{bmatrix} \quad (3)$$

The incremental strain-displacement relation,

$$\Delta e_\xi = \frac{d\Delta u}{d\xi} + \frac{dv}{d\xi}\frac{d\Delta v}{d\xi} + \frac{1}{2}\left(\frac{d\Delta v}{d\xi}\right)^2 - \eta\frac{d^2\Delta v}{d\xi^2} \quad (4)$$

may be written in terms of $\{\Delta d_a\}$ as follows:

$$\Delta e_\xi = \left\{\{B_1\}^T + (\theta + \tfrac{1}{2}\Delta\theta)\{B_2\}^T - \eta\{B_3\}^T\right\}[\Gamma]^{-1}\{\Delta d_a\} \quad (5)$$

where $\{B_1\} = \begin{Bmatrix} 1 \\ 0 \\ 0 \end{Bmatrix}$, $\{B_2\} = \begin{Bmatrix} 0 \\ 2\xi \\ 3\xi^2 \end{Bmatrix}$ and $\{B_3\} = \begin{Bmatrix} 0 \\ 2 \\ 6\xi \end{Bmatrix}$ (6)

The principal cross-sectional properties in elastic and plastic ranges can be simulated by an equivalent idealized sandwich cross-section [7] with a good accuracy. The dimensionless stress-strain relation for each flange with a concentrated area is assumed to be given by

$$\Delta\sigma_\xi = \gamma^*\Delta e_\xi, \quad \textit{where } \gamma^* = 1 \textit{ for an elastic and unloading response and } \gamma^* = \gamma = E_T/E \textit{ for a plastic response.} \quad (7)$$

The dimensionless stress and forces have been nondimensionalized with respect to E and $EA/2$, respectively. The bilinear hysteretic stress-strain relation (7) may be said to be the simplest but crude first approximation in view of the actual hysteretic stress-strain relations of wide-flange steels, but has been utilized in view, firstly of the computational capacity of our currently available computer and secondly of the fairly crude

detection of plastic and unloading responses by means of the mean stress and strain in a flange of an element defined as the respective averages of the end values of the element.

The incremental virtual work equation for an element may be written as:

$$\{\delta\Delta d_a\}^T\{\Delta p_a\} = \sum_{L,U}\left(\int_0^1 \Delta\sigma_\xi \delta\Delta e_\xi d\xi + \int_0^1 \sigma_\xi \Delta\theta_\xi \delta\Delta\theta_\xi d\xi \right) \tag{8}$$

where the sum is to be taken only over the lower and upper flanges of the element for which $\eta = \frac{1}{2}h$ and $\eta = -\frac{1}{2}h$ where $h = H/l$ and H denotes the depth of the element. The integrands of Eq.(8) may be expressed in terms of the vectors $\{B_1\}$, $\{B_2\}$ and $\{B_3\}$ defined by Eq.(6) and, after integration, the element-stiffness equation may be written in the following form:

$$\{\Delta p_a\} = [\kappa]\{\Delta d_a\} = [\Gamma]^{-1T}\left(\sum_{L,U} \gamma^*([A] + [B]) + [C] \right)[\Gamma]^{-1}\{\Delta d_a\} \tag{9}$$

where 3×3 symmetric matrix [A] contains h only and [B] may be expressed in terms of α_2 and α_3 of the current state. [C] contains essentially the current end forces decomposed in the directions of the current local coordinate axes of this element.

The element-stiffness equation (9) is now expanded into the equation in terms of the displacement vector $\{\Delta D\} = \{\Delta U_a\ \Delta V_a\ \Delta\Theta_a \mid \Delta U_b\ \Delta V_b\ \Delta\Theta_b\}^T$ and the force vector $\{\Delta P\} = \{\Delta P_a\ \Delta Q_a\ \Delta R_a \mid \Delta P_b\ \Delta Q_b\ \Delta R_b\}^T$ defined in the global coordinates shown in Fig.4. The relation between $\{\Delta d_a\}$ and $\{\Delta D\}$ may be reduced to the following form:

$$\{\Delta d_a\} = \left[[T_R]^T \mid -[H]^T[T_R]^T \right]\{\Delta D\} \tag{10}$$

where $[T_R]$ and $[H]$ denotes the 3×3 coordinate transformation matrix and the equilibrium matrix respectively. The relation between $\{\Delta P\}$ and $\{\Delta p_a\}$ may be reduced to the following form:

$$\{\Delta P\} = [T]^T\{\Delta p_a\} + [P_a]\{\Delta D\} \tag{11}$$

where

$$[P_a] = \left[\begin{array}{c|c} [0] & \{F_a\} \\ \hline \{F_a\}^T & M_a \end{array}\right] \qquad \{F_a\}^T = \{-Q_a\ P_a\ 0\ Q_a\ -P_a\} \qquad M_a = -q_a v_a - p_a(1+u_a) \tag{11a-c}$$

After substitution of Eqs.(9) and (10) into (11), the resulting equation may finally be reduced to the desired large-displacement incremental element-stiffness equation in the following form:

$$\{\Delta P\} = [\kappa_G]\{\Delta D\} \tag{12}$$

where

$$[\kappa_G] = [[T]^T[\kappa][T] + [P_a]] \tag{12a}$$

Eq.(12) may further be rewritten in terms of the state vectors $\{\Delta S_a\} = \{\Delta U_a\ \Delta V_a\ \Delta\Theta_a \mid \Delta P_a\ \Delta Q_a\ \Delta R_a\}^T$ and $\{\Delta S_b\} = \{\Delta U_b\ \Delta V_b\ \Delta\Theta_b \mid \Delta P_b\ \Delta Q_b\ \Delta R_b\}^T$ to define the field transfer matrix for the element. By applying the standard technique of the transfer matrix method to a member j consisting of several elements, the field transfer matrix in terms of the state vectors at the left and right ends of the member can be derived. The resulting state equation may then be readily converted into the desired incremental member-stiffness equation:

$$\{\Delta P_j\} = [K_j]\{\Delta D_j\} \tag{13}$$

4. EQUATION OF MOTION

Let $\{u\}$ denote the relative nodal displacement vector with respect to the base rock as shown in Fig.2. The displacement vector of the base rock consisting of the horizontal and vertical displacement components is denoted by $\{u_g\}$. The lumped mass matrix $[\,M\,]$ consists of diagonal elements corresponding to all the nodal displacements, including the mass moments of inertia for the joints. The damping matrix $[\,D_I\,]$ consists of the two matrices which are respectively proportional to the stiffness matrices of super- and substructures. Let $[\,K(u)\,]$ denote the system stiffness matrix generated in terms of the current nodal displacements to be used for the subsequent incremental response analysis.

The incremental equation of motion may be written as

$$[\,M\,]\{\Delta\ddot{u}\} + [D_I]\{\Delta\dot{u}\} + [K(u)]\{\Delta u\} = -\,[\,M\,]\{\Delta\ddot{u}_g\} \tag{14}$$

Numerical integration has been carried out by the well-known linear acceleration method in Wilson and Clough's version [8]. In the computation, different values of damping coefficients have been used for the frame and for the base.

5. ENERGY BALANCE

The equation of energy balance may be used as the most significant check on the accuracy of the proposed computational method of analysis. The kinetic energy of the system is given by

$$W_M = \frac{1}{2}\{\dot{u}\}^T[\,M\,]\{\dot{u}\} \tag{15}$$

where $\{\dot{u}\}$ denotes the current nodal velocity vector. The dissipated energy due to viscous damping may be written as

$$W_D = \sum_{n=1}^{N}\left(\sum_{r=1}^{n-1}\{\Delta\dot{u}\}_r^T[D_I]_r + \frac{1}{2}\{\Delta\dot{u}\}_n^T[D_I]_n\right)\{\Delta u\}_n \tag{16}$$

where subscripts r and n affixed to $\{\Delta\dot{u}\}$ and $[D_I]$ denote the increment or the value in the r-th and n-th steps, respectively. The internal work computed from the nodal forces and nodal displacements may be written as

$$W_S = \sum_{n=1}^{N}\left(\sum_{r=1}^{n-1}\{\Delta u\}_r^T[K]_r + \frac{1}{2}\{\Delta u\}_n^T[K]_n\right)\{\Delta u\}_n \tag{17}$$

The input energy due to the ground motion is computed by

$$W_F = \sum_{n=1}^{N}\left(-\sum_{r=1}^{n-1}\{\Delta\ddot{u}_g\}_r^T[\,M\,] - \frac{1}{2}\{\Delta\ddot{u}_g\}_n^T[\,M\,]\right)\{\Delta u\}_n \tag{18}$$

The work done by the dead loads concentrated at the nodes may be written as

$$W_V = \{F_V\}^T\left(\{u\} - \frac{1}{2}\{u_{DEAD}\}\right) \tag{19}$$

where $\{F_V\}$ denotes the nodal force vector representing the dead loads and $\{u_{DEAD}\}$, the static dead load response vector.

The equation of energy balance may then be written as

$$W_M + W_D + W_S = W_F + W_V \tag{20}$$

It should be noted that, W_D, W_S and W_F must be computed as the respective sums of the respective increments up to the current state denoted by the n-th step, and that W_S consists of the elastic strain energy W_E in the

current state and the energy W_P dissipated for the plastic deformation up to the current state.

6. NUMERICAL EXAMPLES

FRAME The dimensions of the model frame and the dead loads are shown in Fig.1. A modified version of the minimum weight design [6], [5] has been applied to design the frame for triangularly distributed lateral loads with base shear coefficient 0.2. The length of an element is 50cm.

GROUND STIFFNESS PROPERTIES Based upon Barkan's method for spring constants of the ground, the coefficient of elastic uniform vertical compression has been assumed to be 0.005 ton/cm^3. The values 0.01 and 0.20 have been taken as the internal viscous damping coefficients for the members and the ground, respectively.

INPUT EARTHQUAKE DISTURBANCES The wave patterns of Vernon S82° E and El Centro NS with the acceleration amplitude 2000 *gal* have been used for the purpose of testing the proposed method if it is able to trace, with a considerably good accuracy, the dynamic deterioration process.

RESPONSE AND DISCUSSION

(1) Time Histories of Energy Quantities (Fig.5,6) The durations of significant energy supplies for the Vernon case and El Centro case were 0.2~1.25sec and 1.0~5.5sec, respectively. While W_V remained negligibly small for the Vernon input, W_V for the El Centro input increased considerably and remained still increasing even after the energy supply became negligibly small. W_M became negligibly small corresponding to the ceasing of the energy supply in both cases. While W_D was greater than W_E, both were negligibly small compared to W_F at large deflection range. The maxima of W_E for the two inputs were almost the same. Apparently most of W_F was dissipated for plastic deformation in large deflection range. Even after W_F ceased to grow, W_V has kept still increasing and W_P has exceeded W_F eventually in the El Centro case. Although this is merely an example, such a circumstance may have to be considered as an indication of the dynamic deterioration of the frame in the sense that W_V and W_P are the significant factors governing the subsequent deformation.

(2) Story shear-story displacement diagrams (Fig.7,8) *and Time Histories of Horizontal displacements* (Fig.9,10) The maximum story shear is about twice the design story shear force in both cases. The variations of the neutral deflected configuration of motion in both cases apparently show that the frame was gradually titled in one derection. It may be noticed that the force-displacement loops are so complicated that any simplified models would not be able to simulate quantitatively this tendency of tilting.

(3) Permanent Deformation (Fig.1) The final configuration of the frame after the El Centro input is shown in Fig.1. The horizontal displacements after the El Centro input and after the Vernon input amounted to 160 cm and 63 cm, respectively.

(4) On the Efficiency of the Program The computation was carried out on an IBM 360-K195 computer. The time required for one incremental step was

about 0.10∿0.12 sec. The computer output has shown that the energy balance equation (20) has been satisfied to the accuracy of 0.4% of $(W_F + W_V)$ at worst, and of less than 0.1% mostly over the whole ranges. The numerical examples obtained with this fast computing time and with this accuracy of the energy check appear to be good evidences of the efficiency of the present method of dynamic large-deflection analysis of strain-hardening frames subjected to strong-motion earthquake disturbances.

7. CONCLUSIONS

(1) An efficient computational method of dynamic large-deflection analysis of multi-story building frames consisting of elastic strain-hardening beams and columns has been proposed. The idea of combining the transfer matrix technique with the usual large-deflection stiffness matrix method and with the automatic generation procedure of sub-elements in each member has been shown to be very effective to reduce the size of computation.

(2) The numerical examples may be said to be good evidences of the efficiency of the method and appear to indicate the possibility of analyzing catastrophic dynamic responses of high-rise building frames of even more than 30 stories with currently available computers.

(3) Although no quantitative conclusions can be drawn from the two examples, the numerical results appear to indicate that the gravity effect has a significant influence upon the deteriorating process and dynamic collapse behavior of strain-hardening multi-story frames.

Acknowledgments The authors would like to thank Mr. K. Nakanishi, Mr. O. Ohta and Mr. Takashi Nakamura for their assistance in the computation and data processing.

REFERENCES

[1] See for instance, T. Kobori, R. Minai and T. Hujiwara, "Response Analysis of R-O type Elastic-plastic Building Frames,"(In Japanese) Annals of Disaster Prev. Res. Inst., Kyoto Univ., Vol.14A, 1971, pp301-313.

[2] R. Husid. "Gravity Effect on the Earthquake Response of Yielding Structures," Ph.D.Thesis, CIT Pasadena, California, June 1967.

[3] R. A. Adu, "Response and Failure of Structures under Stationary Random Excitation", Ph.D.Thesis, CIT Pasadena, California, May 1971.

[4] R.Tanabashi, K.Kaneta, Tsuneyoshi Nakamura and S.Ishida, "To the Final State of Rectangular Frames," Proc.4WCEE, Santiago,Chile, Jan.1969.

[5] R.Tanabashi, Tsuneyoshi Nakamura and S.Ishida, "Overall Force-deflection Characteristics of Multi-story Frames," 1971 Proc. of 1969 Symp. on Ultimate Strength of Structures and their Components, Tokyo, Japan.

[6] R.Tanabashi and Tsuneyoshi Nakamura, "The minimum Weight Design of a Class of Multi-story Frames Subjected to Large Lateral For es I, II" Trans. Archit.Inst.Japan, No.118,Dec.1965 & No.119, Jan.1966, & "An Approach to the Last Hinge point Design of Tall Multi-story Frames," Proc.1964 Symp.Ext.Forces & Str. Design of High-rise & Long-span Str.

[7] Tsuneyoshi Nakamura,"Elastic-plastic Behavior of a Linear Strain-hardening Sandwich Column Subjected to Alternating Lateral Force, Summaries of Tech. Papers of Annual Meeting of A.I.J. 1966, p285.

[8] R.W.Clough, "Analysis of Structural Vibrations and Dynamic Response," RECENT ADVANCES IN MATRIX METHODS OF STRUCTURAL ANALYSIS AND DESIGN, Edited by R.H.Gallagher, Y.Yamada & J.T.Oden, Univ.Alabama Press, 1971.

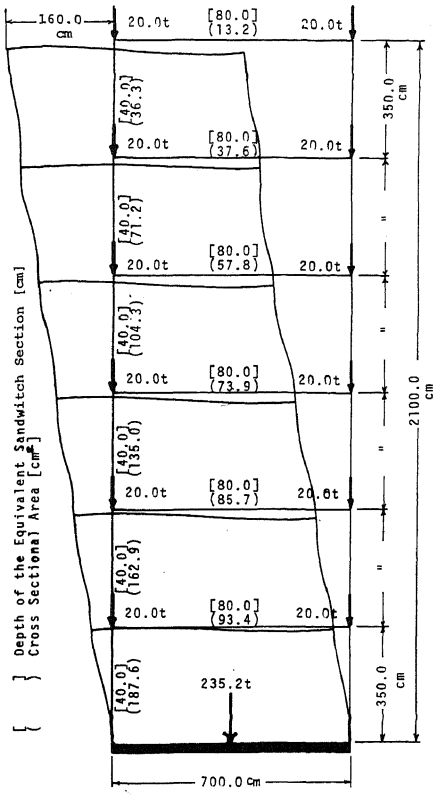

FIG. 1 FRAME DIMENSIONS AND PERMANENT DEFORMATION FOR ELCENTRO EXCITATION

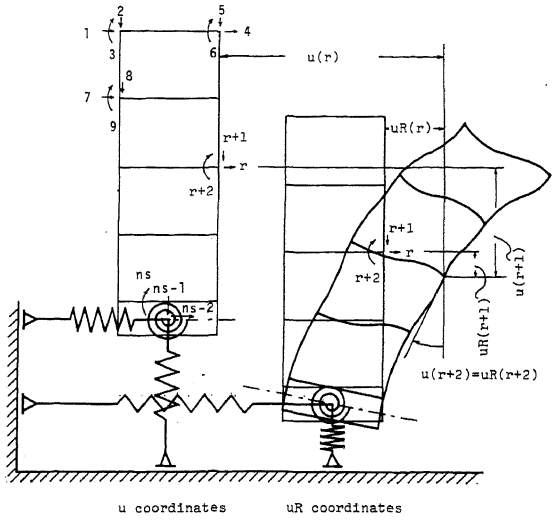

FIG. 2 IDEALIZED FRAME AND COORDINATE SYSTEM

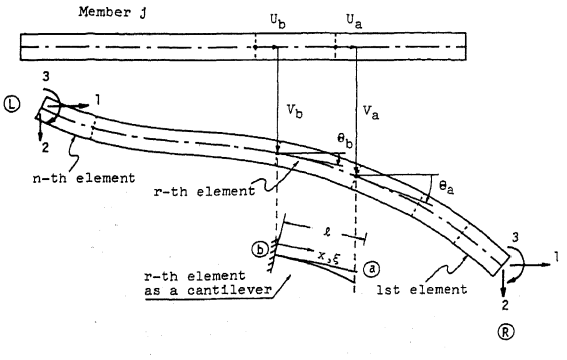

FIG. 3 COORDINATES FOR A MEMBER AND FOR AN ELEMENT

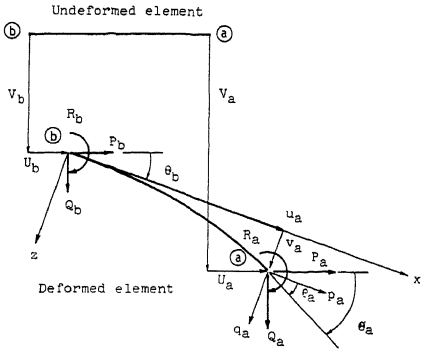

FIG. 4 LOCAL AND GLOBAL COORDINATES FOR AN ELEMENT

FIG. 5 TIME HISTORIES OF ENERGY QUANTITIES FOR VERNON EXCITATION

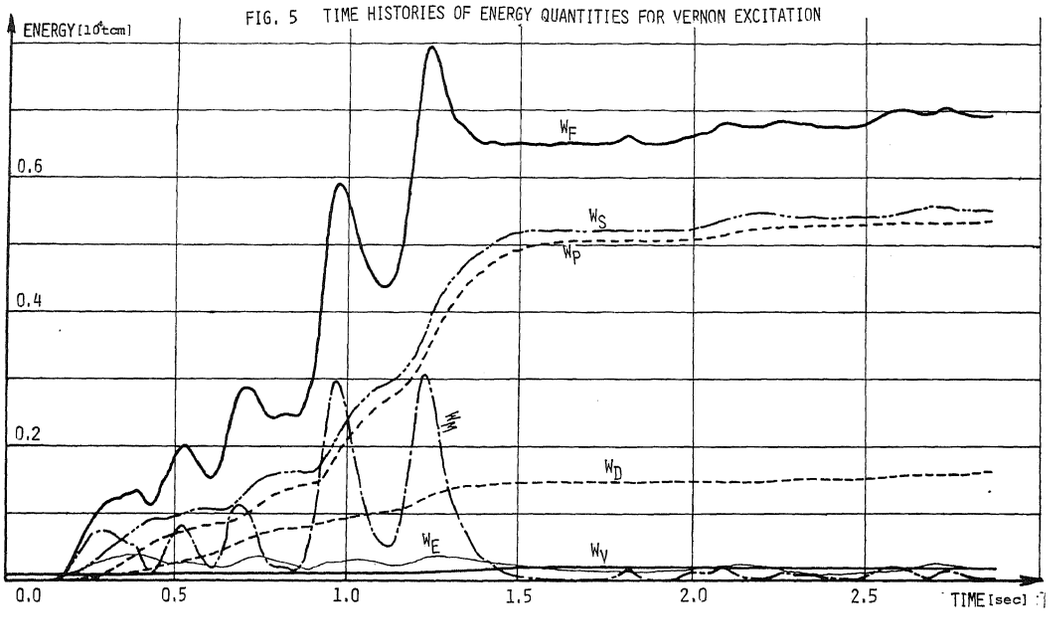

FIG. 6 TIME HISTORIES OF ENERGY QUANTITIES FOR ELCENTRO EXCITATION

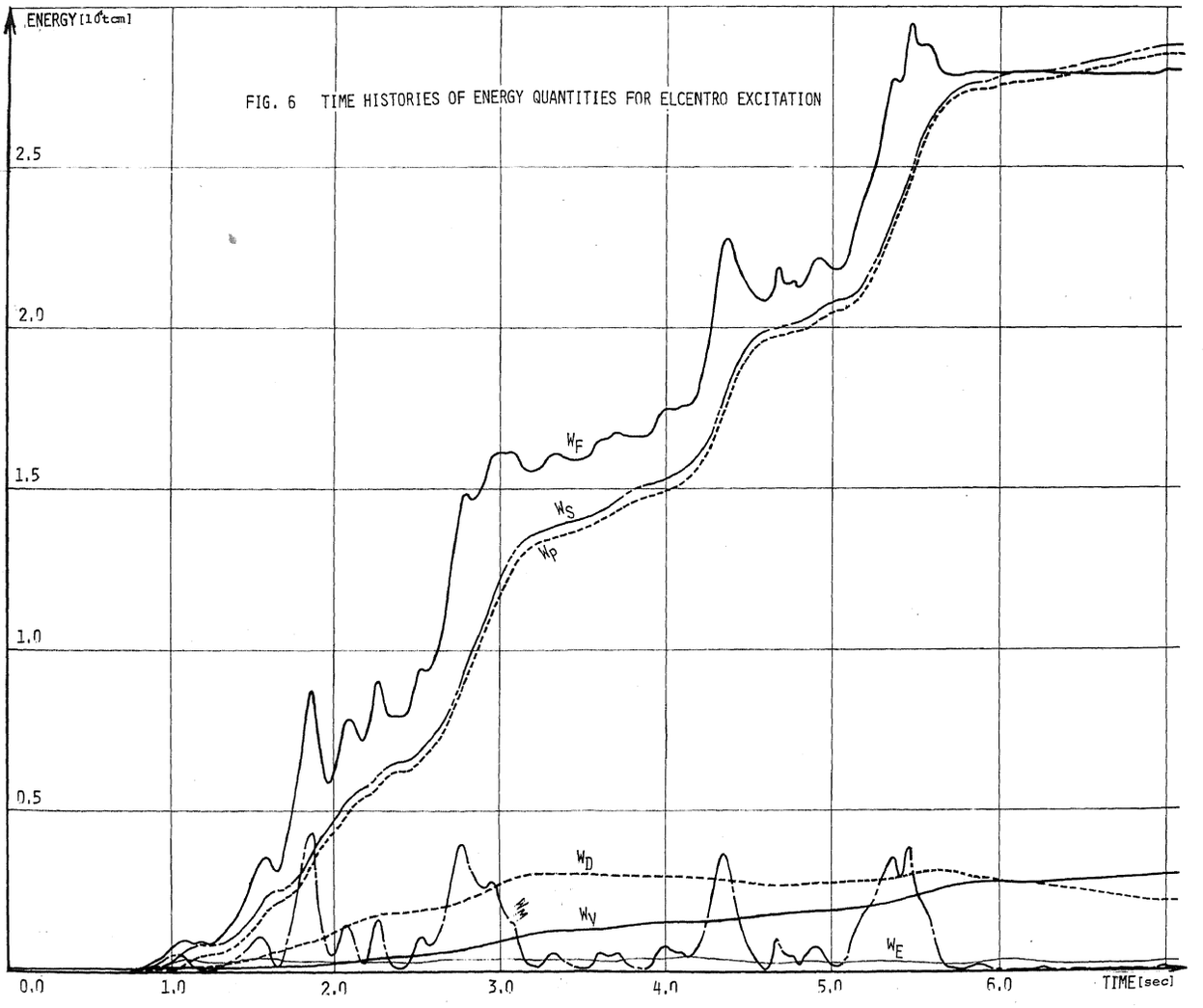

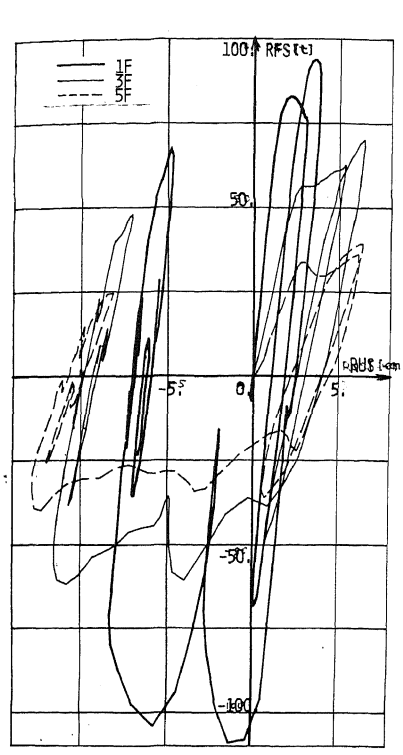

FIG. 7 STORY SHEAR AND STORY DISPLACEMENT DIAGRAM FOR VERNON EXCITATION

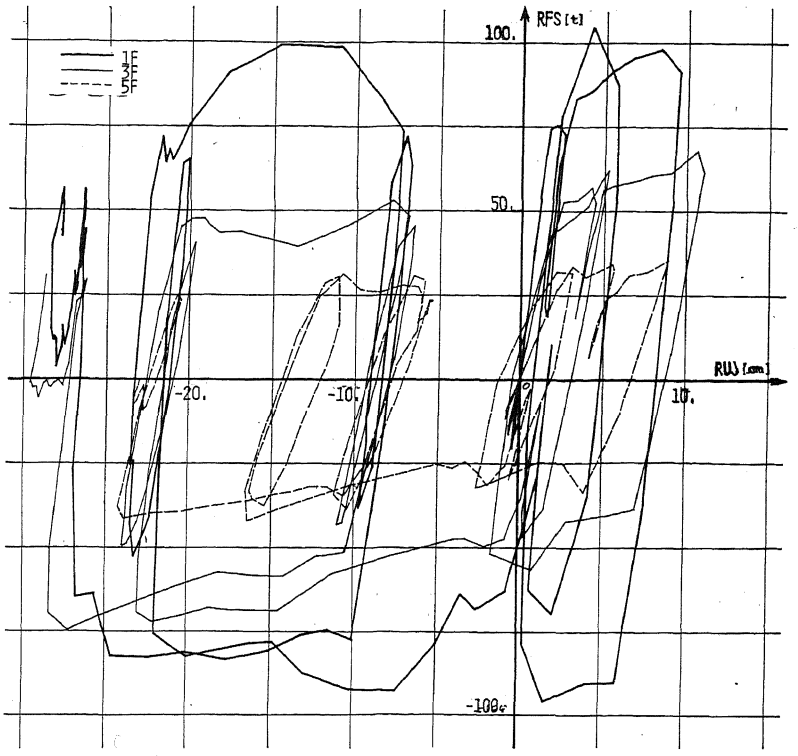

FIG. 8 STORY SHEAR AND STORY DISPLACEMENT DIAGRAM FOR ELCENTRO EXCITATION

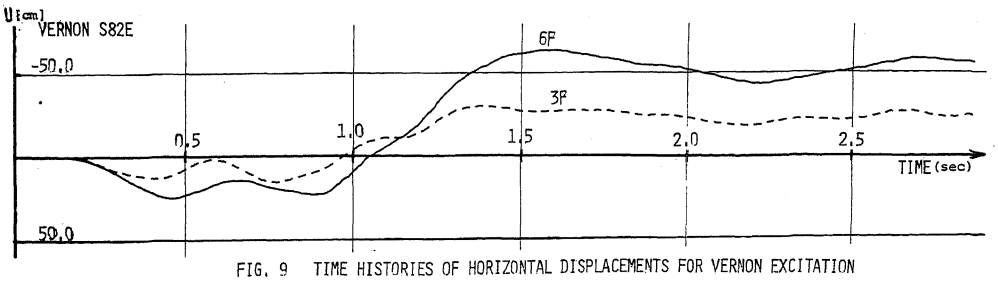

FIG. 9 TIME HISTORIES OF HORIZONTAL DISPLACEMENTS FOR VERNON EXCITATION

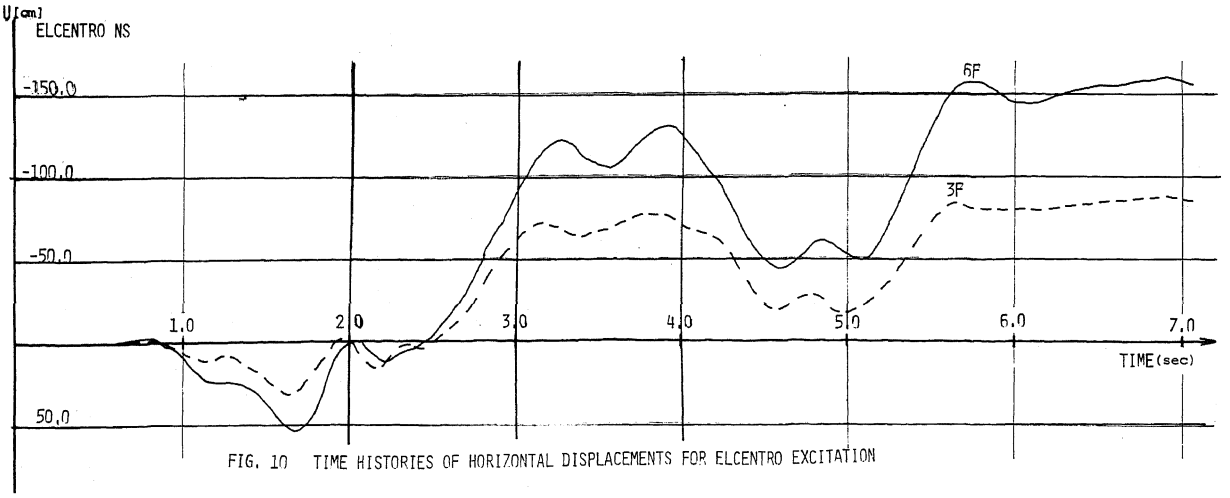

FIG. 10 TIME HISTORIES OF HORIZONTAL DISPLACEMENTS FOR ELCENTRO EXCITATION